AMERICAN SOCIETY FOR MICROBIOLOGY | Journal of Bacteriology®

RESEARCH ARTICLE

Incomplete Hydrogenation by Geranylgeranyl Reductase from a Proteobacterial Phototroph *Halorhodospira halochloris*, Resulting in the Production of Bacteriochlorophyll with a Tetrahydrogeranylgeranyl Tail

Yusuke Tsukatani,[a] Jiro Harada,[b] Kanako Kurosawa,[a] Keiko Tanaka,[a] Hitoshi Tamiaki[c]

[a]Institute for Extra-Cutting-Edge Science and Technology Avant-Garde Research (X-star), Japan Agency for Marine-Earth Science and Technology (JAMSTEC), Kanagawa, Japan

[b]Department of Medical Biochemistry, Kurume University School of Medicine, Fukuoka, Japan

[c]Graduate School of Life Sciences, Ritsumeikan University, Shiga, Japan

ABSTRACT Light harvesting and charge separation are functions of chlorophyll and bacteriochlorophyll pigments. While most photosynthetic organisms use (bacterio)chlorophylls with a phytyl (2-phytenyl) group as the hydrophobic isoprenoid tail, *Halorhodospira halochloris*, an anoxygenic photosynthetic bacterium belonging to Gammaproteobacteria, produces bacteriochlorophylls with a unique 6,7,14,15-tetrahydrogeranylgeranyl (2,10-phytadienyl) tail. Geranylgeranyl reductase (GGR), encoded by the *bchP* gene, catalyzes hydrogenation at three unsaturated C=C bonds of a geranylgeranyl group, giving rise to the phytyl tail. In this study, we discovered that *H. halochloris* GGR exhibits only partial hydrogenation activities, resulting in the tetrahydrogeranylgeranyl tail formation. We hypothesized that the hydrogenation activity of *H. halochloris* GGR differed from that of *Chlorobaculum tepidum* GGR, which also produces a pigment with partially reduced hydrophobic tails (2,6-phytadienylated chlorophyll *a*). An engineered GGR was also constructed and demonstrated to perform only single hydrogenation, resulting in the dihydrogeranylgeranyl tail formation. *H. halochloris* original and variant GGRs shed light on GGR catalytic mechanisms and offer prospective bioengineering tools in the microbial production of isoprenoid compounds.

IMPORTANCE Geranylgeranyl reductase (GGR) catalyzes the hydrogenation of carbon–carbon double bonds of unsaturated hydrocarbons of isoprenoid compounds, including α-tocopherols, phylloquinone, archaeal cell membranes, and (bacterio)chlorophyll pigments in various organisms. GGRs in photosynthetic organisms, including anoxygenic phototrophic bacteria, cyanobacteria, and plants perform successive triple hydrogenation to produce chlorophylls and bacteriochlorophylls with a phytyl chain. Here, we demonstrated that the GGR of a gammaproteobacterium *Halorhodospira halochloris* catalyzed unique double hydrogenation to produce bacteriochlorophylls with a tetrahydrogeranylgeranyl tail. We also constructed a variant enzyme derived from *H. halochloris* GGR that performs only single hydrogenation. The results of this study provide new insights into catalytic mechanisms of multiposition reductions by a single enzyme.

KEYWORDS anoxygenic photosynthetic bacteria, bacteriochlorophyll, geranylgeranyl reductase, isoprenoid, pigment biosynthesis, *Chlorobaculum tepidum*, *Halorhodospira halochloris*, chlorophyll, photosynthesis, purple bacteria

Chlorophyll (Chl) and bacteriochlorophyll (BChl) pigments are critical in photosynthetic organisms for harvesting light energy and transferring it to photochemical reaction center (RC) complexes, where the charge separation takes place. Chl occurs in

Editor Conrad W. Mullineaux, Queen Mary University of London

Address correspondence to Yusuke Tsukatani, tsukatani@jamstec.go.jp.

The authors declare no conflict of interest.

Received 10 December 2021
Accepted 19 January 2022
Accepted manuscript posted online 28 February 2022
Published 15 March 2022

all oxygenic phototrophs (including plants, algae, and cyanobacteria) and some species of anoxygenic phototrophic bacteria with type-I RCs (1–3). In the green sulfur bacterium *Chlorobaculum tepidum*, Chl is attached to type-I RCs and functions as the primary electron acceptor A_0, although BChls are major pigments in the bacterium (2). BChl pigments are detected in all species of anoxygenic phototrophic bacteria, regardless of whether they have type-I or type-II RCs, but not in oxygenic phototrophs.

Photosynthetic organisms biosynthesize pigments through a series of catalytic reactions by various enzymes (4, 5). Chl and BChl share early biosynthetic steps, from an initial substance 5-aminolevulinic acid to chlorophyllide *a* or divinyl chlorophyllide *a* (4–7). The committed biosynthetic step for BChl *a* is branched at the chlorophyllide *a* reduction stage (6), whereas the committed step for BChl *b* and BChl *g* is branched at the 8-vinyl chlorophyllide *a* (7–9). These two steps correspond to the conversion of a chlorin ring into a bacteriochlorin ring.

Although Chl and BChl species possess specific core π-skeletons and peripheral substituents, the penultimate and last biosynthetic steps for all the photosynthetic (B)Chl pigments except Chl c are common, where the order of the two steps can be switched. The esterification of geranylgeranyl diphosphate into the substituent at the carbon 17 (C17) position of (bacterio)chlorophyllide (10–12) is the penultimate step. The esterification is catalyzed by an enzyme designated as (B)Chl synthase encoded by the *bchG/chlG* gene. The last step is the hydrogenation of the C17 geranylgeranyl to the phytyl tail, which is catalyzed by *bchP/chlP* gene-encoded geranylgeranyl reductase (GGR) (10, 13). As depicted in Fig. 1, the geranylgeranyl tail is reduced three times to a phytyl group. The triple double-bond reduction of geranylgeranyl group by GGR occurred in the order of C10=C11, C6=C7, and C14=15 (Fig. 1, left column) (14).

Halorhodospira halochloris, a halophilic anoxygenic phototrophic bacterium belonging to the phylum Gammaproteobacteria, produces BChl *b* esterified with a unique isoprenoid tail at the C17 position, namely, a tetrahydrogeranylgeranyl (THGG) tail (Fig. 1, middle column) (15, 16). The THGG tail in *H. halochloris* is characterized as the C10=C11 unreduced double bond (thereby also called 2,10-phytadienyl) (15, 16), indicating that the first double-bond reduction of the triple hydrogenation occurring in other phototrophic bacteria is likely skipped or inhibited *in vivo* in *H. halochloris* (Fig. 1, middle). Therefore, the following two hypotheses emerge: (i) GGR in *H. halochloris* only reduces the isoprenoid tail twice, or (ii) GGR in *H. halochloris* potentially reduces three times, as observed in other phototrophic bacteria, but is prevented from reducing the C10=C11 double bond by an unidentified component(s). The latter case has been proposed for Chl biosynthesis in green sulfur bacteria (17, 18).

Green sulfur bacteria produce BChl *a* with the usual phytyl tail, but they also produce Chl *a* esterified with a unique THGG group (Fig. 1, right column) (2, 19). The hydrophobic THGG tail of Chl *a* in *C. tepidum* displays the C6=C7 unreduced double bond (2), which is different from the C10=C11 unreduced double bond in *H. halochloris* (Fig. 1). In the case of *C. tepidum*, a mutant lacking GGR accumulated BChl *a* and Chl *a* with the geranylgeranyl tails at the C17 position (17, 18), and it was concluded that a single *bchP* gene, *CT2256*, is responsible for saturating the geranylgeranyl tails esterified with both BChl *a* and Chl *a* in *C. tepidum*. Therefore, GGR (gene product of *CT2256*) of *C. tepidum* potentially has a catalytic ability of three reductions of the geranylgeranyl moiety, yielding the phytyl tail; however, this ability is somehow inhibited or unachieved in Chl biosynthesis but not in BChl biosynthesis. This *C. tepidum* GGR model correlates with the aforementioned second hypothesis. Recently, through an analysis of whole-genome sequencing of *H. halochloris*, a *bchP* gene was identified in the photosynthetic gene cluster of its genome (20). In this study, we investigated the catalytic activities of the *H. halochloris* GGR by creating a series of complementation mutants.

RESULTS

We first constructed the Δ*bchP* mutant of *R. sphaeroides* lacking GGR (Fig. 2) (for details, see Materials and Methods). The Δ*bchP* mutant strain served as a host to

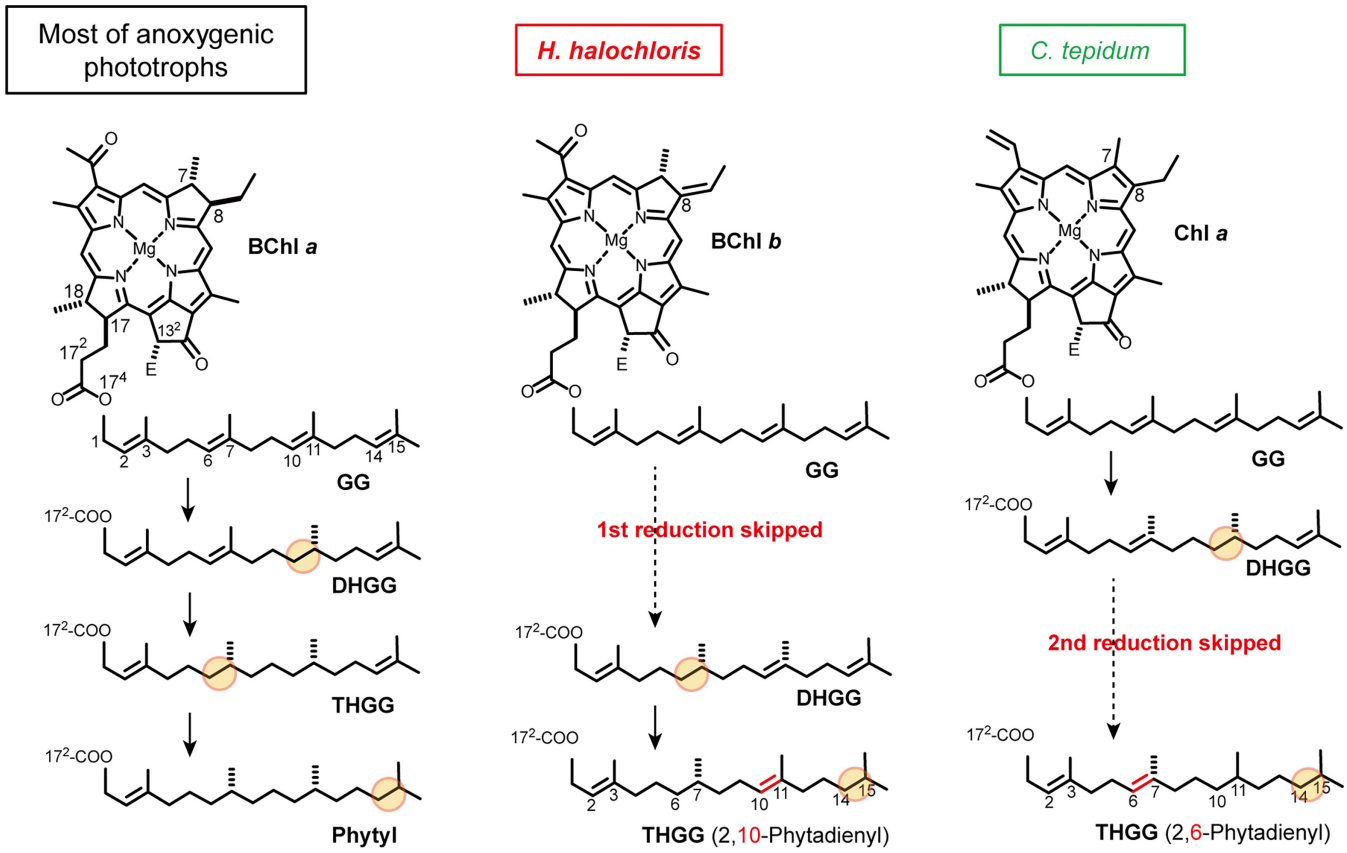

FIG 1 Reaction schemes for hydrogenation processes from the GG tail in (B)Chl biosynthesis. (Left panel) Proposed hydrogenation steps for phytyl formation in most phototrophic bacteria producing BChl a_P. (Middle panel) Proposed hydrogenation steps for THGG formation in *H. halochloris* producing BChl b_{THGG}. Note that BChl *a* has an ethyl group at the C8 position, whereas BChl *b* has a C8 ethylidene group. (Right panel) Proposed hydrogenation steps for THGG formation in *C. tepidum*, which produces Chl a_{THGG}. "E" at the $C13^2$ position represents $COOCH_3$.

construct complementation mutants containing wild-type and variant GGRs of *H. halochloris* and *R. sphaeroides*. We examined the pigment compositions of these mutant strains using high-performance liquid chromatography (HPLC) (Fig. 3). The HPLC elution profile of pigment extracts from the wild type of *R. sphaeroides* revealed an authentic phytylated BChl *a*, which was eluted at roughly 20.5 min (Fig. 3, profile 1). The Δ*bchP* mutant of *R. sphaeroides* lacking GGR did not exhibit the phytylated BChl *a* profile at 20.5 min; instead, the mutant accumulated geranylgeranylated BChl *a*, which was eluted at roughly 14.5 min (Fig. 3, profile 2). Profile 3 in Fig. 3 depicts the HPLC elution profile of pigment extracts from *Rhodopseudomonas* sp. strain Rits, which was discovered to accumulate BChl *a* molecules with unreduced and partially-reduced isoprenoid tails (14, 21). *Rhodopseudomonas* sp. strain Rits exhibited four elution peaks at 14.5, 16, 18, and 20.5 min, which were attributed to BChl *a* esterified with GG, dihydrogeranylgeranyl (DHGG), THGG, and phytyl tails, respectively, according to the previous study (21) (Fig. 3, profile 3). The HPLC elution profile of pigments extracted from the Hh_P_wt mutant, which has an intact GGR of *H. halochloris* in the background of the *R. sphaeroides* Δ*bchP* strain, revealed three peaks of BChl *a* esterified with GG, DHGG, and THGG tails (Fig. 3, profile 4), but no phytylated BChl *a*. The result indicates that the GGR of *H. halochloris* catalyzes only two double-bonds hydrogenation, and thereby the final product has the THGG tail, rather than the phytyl tail. Although both organisms produce (B)Chl pigments with THGG tails, the potential catalytic activity of *H. halochloris* GGR differs from that of *C. tepidum* GGR (17, 18). *C. tepidum* produces Chl *a* with the THGG tail, but Harada et al. showed that a mutant complemented with *C. tepidum* GGR produced phytylated BChl *a*, indicating that *C. tepidum* GGR can reduce a GG tail attached to a bacteriochlorin ring to a phytyl tail (17).

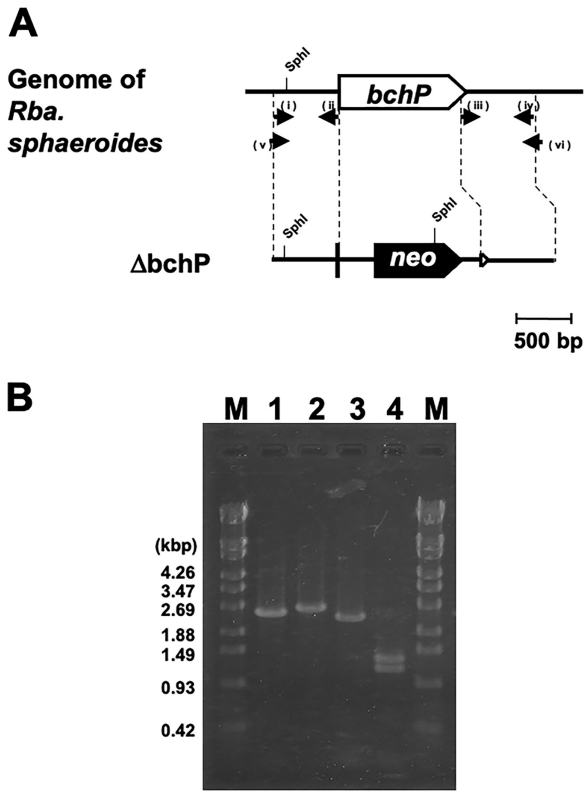

FIG 2 Construction of Δ*bchP* mutant as the host for complementation experiments. (A) Schematic drawing of the *bchP* locus of *R. sphaeroides*. The *bchP* gene was inactivated by replacement with the *neo* gene conferring resistance to kanamycin. Arrows represent the primers that were used in this study: (i) bchPus-F, (ii) bchPus-R, (iii) bchPud-F, (iv) bchPud-R, (v) sphaP-comf-F, and (vi) sphaP-comf-R. (B) Analytical PCR of the *bchP* locus of the wild-type and mutant *R. sphaeroides*. Using sphaP-comf-F and -R primers, the amplified PCR products from wild-type and *bchP*-deletion mutant strains are estimated to be 2.48 and 2.66 kbp, and were loaded onto lanes 1 and 2, respectively. Because of the length differences between the two PCR fragments, these were then digested by the restriction enzyme, SphI. The length of the digested PCR products from the wild type remained nearly unchanged (approximately 0.15 and 2.33 kbp, lane 3), whereas the PCR fragments from the *bchP* mutant were digested into three pieces (approximately 0.15, 1.17, and 1.34 kbp, lane 4). The DNA molecular weight marker, λ-EcoT14I digest (TaKaRa-Bio), was used to estimate the molecular mass of PCR products in lane M.

Figure 4 depicts the N-terminus of the amino acid sequence alignment of GGR from several phototrophic bacteria and nonphotosynthetic archaea. *H. halochloris* GGR has a characteristic insertion at the N-terminal side of its primary sequence (Fig. 4, colored in red). We constructed the Δ*bchP* mutant of *R. sphaeroides* complemented with the variant GGR of *H. halochloris* that lacks the insertion region, designated Hh_P_del, because the insertion region could be relevant to presumably inhibiting the unachieved double-bond reduction at the C10=C11 position. The HPLC elution profile of pigments from the Hh_P_del mutant exhibited the GG peak eluting at roughly 14.5 min and the DHGG peak at around 16 min; however, the mutant did not accumulate peaks derived from BChl *a* with THGG and phytyl tails (Fig. 3, profile 5). The result indicates that the loss of the insertion region of *H. halochloris* GGR caused the loss of either the first or last hydrogenation and that the variant GGR catalyzes only a single hydrogenation reaction, yielding the DHGG tail.

We constructed a positive-control complementation mutation by introducing the intact *bchP* gene for *R. sphaeroides* GGR in the Δ*bchP* mutant of *R. sphaeroides* (designated as Rs_P_wt). The positive-control mutant restored the production of phytylated BChl *a*, as the HPLC elution peak of the pigment was observed at 20.5 min (Fig. 3, profile 6).

In a converse experiment to the Hh_P_del mutant, we constructed a mutant with a modified *bchP* gene, in which the characteristic insertion sequences encoding PAPGVALPPDAKDG

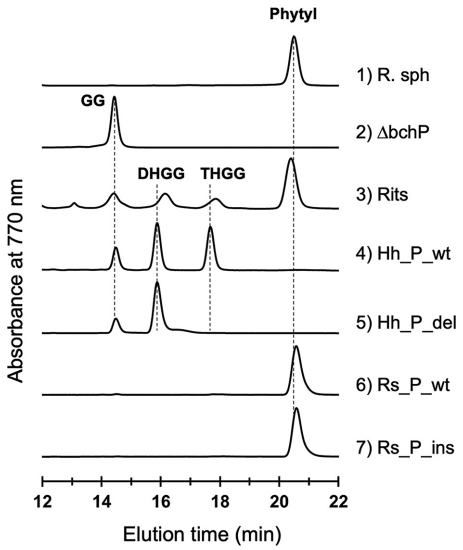

FIG 3 Reverse-phase HPLC elution profiles of pigment extracts from the wild-type and mutant strains. Pigments were extracted from 1) *R. sphaeroides* J001, 2) Δ*bchP* mutant, 3) *Rhodopseudomonas* sp. strain Rits, 4) Hh_P_wt, 5) Hh_P_del, 6) Rs_P_wt, and 7) Rs_P_ins.

(Fig. 4, colored in red) derived from *H. halochloris* were inserted into the corresponding region of *R. sphaeroides bchP* gene. The mutant designated Rs_P_ins accumulated phytylated BChl *a* (Fig. 3, profile 7), which was consistent with the result observed for the Rs_P_wt strain.

DISCUSSION

It has been unknown whether a single GGR enzyme (BchP) in *H. halochloris* is responsible for the unusual THGG tail formation, or whether *H. halochloris* GGR can catalyze phytyl formation as observed in most phototrophs, but unknown protein(s) are involved in inhibiting the C10=C11 reduction in this bacterium. Here, we demonstrated that the heterologous expression of *H. halochloris* GGR in the *R. sphaeroides* mutant lacking its original GGR resulted in the accumulation of BChl *a* esterified with a THGG group. The results indicate that the GGR of *H. halochloris* itself is responsible for the production of the THGG moiety and that the enzymatic activity of GGR in the bacterium is distinct from that in most other phototrophic bacteria producing phytylated BChl *a*.

C. tepidum, a green sulfur bacterium, produces Chl *a* esterified with the THGG moiety, although it also biosynthesized BChl *a* with a regular phytyl tail. The THGG moiety detected in *C. tepidum* is 2,6-phytadienyl and therefore differs from 2,10-phytadienyl in *H. halochloris* (for structural comparison, see Fig. 1). Before recent studies, it had been assumed that *C. tepidum* has two GGRs: one catalyzes phytyl formation in BChl *a* biosynthesis, and another catalyzes THGG formation in Chl *a* biosynthesis. However, Harada et al. constructed a *C. tepidum* mutant lacking the single *bchP* gene (CT2256) and showed that the mutant accumulated BChl *a* and Chl *a* both esterified with the GG group (17). This indicated that there is only one *bchP* gene responsible for GG reduction in the pigment biosynthesis of *C. tepidum* (17, 18). Harada et al. also made complementation experiments and introduced CT2256 into *R. capsulatus* strain lacking its authentic GGR. The *R. capsulatus* mutant was verified to produce phytylated BChl *a* (17). These indicated that GGR (gene product of CT2256) of *C. tepidum* exhibits potentially catalytic activities to reduce GG to phytyl moiety. By contrast, when it reacts with Chl a_{GG}, the reduction of the C6=C7 double-bond of the isoprenoid tail is somehow inhibited or at least unachieved. In this study, we demonstrated that the GGR of *H. halochloris* itself is responsible for the THGG formation and that it has partial, unusual hydrogenation activities lacking the function of the C10=C11 double-bond reduction. Therefore, we conclude that the model proposed for *C. tepidum* GGR differs from that

```
H. halochloris            MP---VANNSADQFDVAVVGGGPAGATAAHYLARQGWSVAMIDRP--GRIK--P--CGGLIPPQLIRE-FDIPF---DLIAANVR  72
H. halophila              M--LMNHSQNAERFDVAVVGGGPAGATAARHLAQQGHEVLLLDRP--GRIK--P--CGGAIPPRAVQD-FEIPD---DMICATVG  73
Ect. haloalkaliphila      -------MAETQTFDIVVVGGGPAGATAANDQARAGRKVLLLDRG--GRIK--P--CGGAIPPVTMTE-FDLPE---SVLVAKIR  68
Alc. vinosum              -------MSNLETFDVVVIGGGPAGATAANDLAKAGRSVCLLDRA--GRIK--P--CGGAIPPQAMRD-FDLPE---SVLANRVS  68
Tfc. mobilis              -------MSNLESYDAVVVGGGPAGATAATELARAGRRVLMLDRA--GRIK--P--CGGAIPPRLIRD-FAIPE---SLLAARVT  68
Rvi. gelatinosus          --------MQLETFDVVVVGGGPAGATAATEIARQGRSVLLLDRA--GRIK--P--CGGAIPPRAIRD-FGIPD---ELIVAKAL  67
Phs. molischianum         -------MTDLKTFDAVVVGGGPAGATAATHLARRGFSVLLLDRA--GRIK--P--CGGAVPPRLMAE-FEIPD---SLLVARIT  68
Rsp. rubrum               MDAVVATQTPAEVFDVVVVGGGPAGATAATDLARAGRRVALLDPE--GRPK--P--CGGAIPPRLMSE-FAIPD---DLPCAQVS  75
Rps. palustris            M------SENSAIYDVIVVGGGPSGATAACDLARAGKRVVLLDRA--GRIK--P--CGGAIPPRAIRD-FAIPD---SMLVAKIN  69
Blc. viridis              -------MSGHETFDVVVVGGGPAGATAATDLARRGHSVLLLDRA--GRIK--P--CGGAIPPRAMRD-FDIPE---SQLVAKVT  68
Blc. tepida               -------MSGHETFDVVVVGGGPAGATAATDLARRGHTVLLLDKA--GRIK--P--CGGAIPPRAIRD-FEIPD---SQIVAKVT  68
R. sphaeroides            -----------MAYDVFVVGGGPSGATAADELARAGKSVALLDRA--GRIK--P--CGGAIPPRLIED-FDIPD---SQIVARIR  64
Rvu. sulfidophilum        -----------MIYDVVVVGGGPAGATAAEDLARSGKKVALLDRE--GRIK--P--CGGAIPPRLMRD-FNISD---EQLVAKID  64
Rsb. denitrificans        ------------MYDVVVIGGGPSGATAALDLVHSGHRVALLDRK--GRIK--P--CGGAIPPRLMQD-FHIGD---DQLLAKVN  63
Erb. longus               --------MTDKIYDAVVVGGGPAGSTAATELALEGHSVLLMERG--GRIK--P--CGGAVPPRLLED-FDIPQ---SLLVAKAR  67
C. tepidum                -----------MLYDVAIIGGGPSGAAAAEILARAGHSTILIERNL-ANVK--P--CGGAIPLGLIEE-FDIPD---ELVEKKLT  65
Cfl. aurantiacus          -----------MAPRVLIVGASVGGATAAITLRSFGIETIMLEKEL-SKAK--P--CGGAVPPAAFRE-FDLPT---SLIDRKVK  65
Rof. castenholzii         ------------MEPVLVVGASVGGATAADTLARAGVPVVMLERDT-SYVK--P--CGGAVPPVAFTE-FDLPE---TLISRKVH  64
Synechocystis 6803        -----------LVLRVAVVGGGPAGSSAAEILVKAGIETYLFERKL-DNAK--P--CGGAIPLCMVDE-FDLPP---EIIDRRVR  65
Synechococcus 7942        -----------LALRVAVVGGGPAGSCAAETLVKAGIETYLIERKL-DNAK--P--CGGAIPLCMVSE-FDLPA---EIIDRRVR  65
Synechococcus 7002        -----------MVLRVAVVGGGPAGSSAAEILAKAGIETYIFERKL-DNAK--P--CGGAIPLCMVDE-FDLPP---EIIDRRVR  65
Sulfolobus acidocaldarius --------LKELKYDVLIIGGGFAGSSAAYQLSRRGLKILLVDSKPWNRIGDKP--CGDAVSKAHFDK-LGMPYPKGEELENKIN  74
Archaeoglobus fulgidas    ------------MYDVVVVGAGPAGSMAAKTAAEQGLKVLLVEKR--QEIGT-PVRCAEGISRESIEKFFEVDK---KWIAAEVT  67
Thermoplasma acidophilum  -----------------VVGGGPGGSTAARYAAKYGLKTLMIEKR--PEIGS-PVRCGEGLSKGILNE-ADIKAD-RSFIANEVK  63

H. halochloris            GARIISPTHRH-ADMDIPAPGVALPPDAKDGPLSMLSMVDREVFDEWLRKRATQAGADRRDGKFTSLTQ---DGEGV-LIEYQEG  152
H. halophila              SARMVSPSDRH-VDMPI--------------QDGYVGMVDREVFDEWLRSRAAEAGAQRRDATFKHLEE---GDGGV-YIRYAQG  139
Ect. haloalkaliphila      CARMFSPKDRK-VDMPI--------------QGGYVGMVDRKTFDEWLRKRAAEGGAERRTGTYERIDR---DSDGTAIVRYKDE  135
Alc. vinosum              SARMISPSDRK-VDMPI--------------QNGYVGLVDREHFDEWLRARAAESGATRRTGTFEKIER---DTDGTAIVVYRPG  135
Tfc. mobilis              SARMVSPAGRK-VDMPI--------------DGGYVGMVDRDVFDEWLRARAVQVGTERVTGDFERLHH---DEDGQVTVDYRVT  135
Rvi. gelatinosus          CARMISPTDVK-VDIHI--------------ENGYVGLVDREQFDEWLRERARQCGAVRRTGTFERIDR---DADGCAIVRYRPH  134
Phs. molischianum         KARMIAPSNQH-VDIPI--------------EGGYVGMVNRSTFDEWLRERARTAGAERRTGTFETFER---DENGVAVIRYKDA  135
Rsp. rubrum               GARALAPSGRV-VDMPI--------------TGAVVSMVDRAVFDPWLRARAHQAGACRLHGRFEGFDR---QEDGALVVLWRP-  141
Rps. palustris            AARMVSPSDVE-VDMPI--------------GDGFVGMVDREHFDEWLRKRAASVGAERRTGLFRSFTR---DESGVNTVHYEER  136
Blc. viridis              AARMVSPSNKE-VDMPI--------------EDGYVGMVDRETFDEWLRERAAKAGATRRAGSFERLDR---DSDGVALVRYLP-  134
Blc. tepida               AARMVAPSNKE-VDMPI--------------EDGYVGMVDRATFDEWLRERAAQSGAERRAGTFERIDR---DSDGVALVRYQP-  134
R. sphaeroides            TARMISPTGRK-VDIPI--------------EGGFVGMVDREHFDEWLRRRAAKAGAERLTGTFLRVER---DSFHT-YVVWRE-  129
Rvu. sulfidophilum        TARMISPSGRF-VDIPI--------------ENGFVGMVDRKDFDPFLRARAERAGATRFTGTFVRVER---EEEKT-FLVFRD-  129
Rsb. denitrificans        TARMISPTGRK-VDIPI--------------ENGFVGMVDRKDFDPFLRQRAADAGADYFTGTFVRIER---PEGTP-VVIYRD-  128
Erb. longus               CARMIAPSGRA-VDMPV--------------GETGYVGMVDREDFDEWLRERAVECGAERLTATFEKIER---DDEAHPLVAFRR-  134
C. tepidum                RMSVRSPKGET-IFMHM--------------PNGYVGMVRRERFDRYLREKAQKAGAEVVEALVKKIER---SVDRF-TLQLFN-  130
Cfl. aurantiacus          QCLIVSPSGQE-TRVPV--AG------TIPSDDDYVAMVRREVFDSFLRQRAQERGADLIHAQLTGLRV---DRRGV-VATYRT-  136
Rof. castenholzii         HALVHSPSERV-VEIEV--AG------VHRSDQDYIAMCCREEFDCYIRQRAVQHGATLIEGQLIDLAF---DKEGV-TVTYRE-  135
Synechocystis 6803        KMKMISPSNIE-VNIGQ-----------TLKDDEYIGMCRREVLDGFLRERAEKLGTKVINGTVYKLDIPSKDSDPY-TLHYADH  137
Synechococcus 7942        NMKMISPSNRE-VNINL-----------D-NADEYIGMTRREVLDGFLRDRAAKLGTKLINGTLFRLELPKGDRDPY-VLHYADH  136
Synechococcus 7002        KMKMISPSNIE-VNIGQ-----------TLKDDEYIGMCRREVMDSFMRNRAADLGATLINGTVFKLEIPNNNTDPY-VLHYSDH  137
Sulfolobus acidocaldarius GIKLYSPDMQT-VWTVN--------------GEGFE--LNAPLYNQRVLKEAQDRGVEIWDLTTAMKPI---FEDGY-VKGAVLF  138
Archaeoglobus fulgidas    GAKIYAPNKTE-IVMSEEMAG---------NEVGYV--LERKIFDRHVARLAAKAGAEVYVKTAMVDFE---RKDGK-VK-VKL-  134
Thermoplasma acidophilum  GARIYGPSEKRPIILQSEKAG---------NEVGYV--LERDKFDKHLAALAAKAGADVWVKSPALGVI---KENGK-VAGAKI-  132
```

FIG 4 Partial alignments of the N-terminal region of GGR from various bacteria and archaea, including phototrophic members of Proteobacteria, Chlorobi, and Chloroflexi. The alignment was constructed using the MAFFT program (30) implemented in the Geneious Prime software (31). The characteristic

(Continued on next page)

of *H. halochloris* GGR. In terms of catalyzing hydrogenation of the GG moiety only twice, the GGR of *H. halochloris* is likely to exhibit a novel catalytic mechanism and will provide insights into protein engineering. Additionally, the GGR variant, in which the N-terminal insertion peptides specific for *H. halochloris* were omitted (Hh_P_del), showed another-type partial activity catalyzing only a single hydrogenation reaction (Fig. 3, profile 5). The variant somehow acquired a novel reaction mode, which differs from the original GGR of *H. halochloris*.

Generally, GGR catalyzes the hydrogenation of carbon-carbon double bonds of unsaturated hydrocarbons to produce the corresponding single bond and works in various biosynthetic pathways for isoprenoid products, including α-tocopherols, phylloquinone, and archaeal cell membranes. One of the big enigmas on the catalytic mechanism of GGR is whether multiple hydrogenation reactions are successively conducted without releasing the substrate intermediates, or whether the intermediates (DHGG/THGG tails) dissociate from GGR before the next hydrogenation. The crystal structures of archaeal GGR from *Sulfolobus acidocaldarius*, including GGR bound to the substrate geranylgeranyl pyrophosphate, have been determined (22). In the 3D structure, the substrates were detected at three positions within GGR, although there is an active site in the vicinity of a single FAD. Therefore, it seems that the two observed substrates other than the one closest to the FAD were caught at binding pockets before or after hydrogenation reactions. In addition to site-directed mutation studies, the structure study of archaeal GGR has proposed the catalytic mechanism that the first and second hydrogenation might be processive and that the last third hydrogenation is probably not processive (22). The characteristic insertion of *H. halochloris* GGR (Fig. 4) is probably located close to the binding site that is relevant to the first and second hydrogenation in the archaeal GGR, according to the alignment of primary structures. Asparagine 90 and glycine 91 of *S. acidocaldarius* GGR (Fig. 4, colored in green) located in the vicinity of the pyrophosphate moiety of the substrate geranylgeranyl pyrophosphate (22) are at a similar position to the insertion region of *H. halochloris* GGR in the alignment (Fig. 4). We also performed protein structure prediction with AlphaFold for GGR of *H. halochloris* (Fig. 5). In the predicted structure, the characteristic insertion region constitutes a loop structure in the vicinity of the substrate binding site closest to FAD (Fig. 5B). These results could support the phenomenon that *H. halochloris* lacks hydrogenation at the C10=C11 position, which is probably the first hydrogenation event in other phototrophs, and that the variant GGR of Hh_P_del mutant lacks two hydrogenations, which are probably the first and second ones. However, we could not determine whether the DHGG moiety in the Hh_P_del mutant was a 2,6,10- or 2,10,14-phytatrienyl group. To determine the position of the unreduced double bond, a large number of pigment materials for analysis and the chemical standards of those intermediates are required. Further analysis on this will be reported elsewhere.

Using *Rhodobacter* species, *Rhodopseudomonas* species, barley, and radish sprouts, the order of the three hydrogenations by GGR was previously determined to be C10=C11, C6=C7, and then C14=15 (14) (see Fig. 1). Therefore, in the case of *H. halochloris*, the unachieved hydrogenation at the C10=C11 double bond corresponds to the first reaction (Fig. 1). In this study, the elution peaks of BChl a_{DHGG} and BChl a_{THGG} from mutants having *H. halochloris* GGRs were eluted slightly earlier than those prepared from *Rhodopseudomonas* sp. Rits strain (Fig. 3, profiles 3, 4, and 5). Mizoguchi et al. have reported HPLC elution profiles of BChl *b* esterified with two types of THGG moieties, namely, 2,10- and 2,14-phytadienyl tails, where BChl b_{THGG} with a 2,10-phytadienyl tail eluted slightly earlier than BChl b_{THGG} with a 2,14-phytadienyl tail (16). Similarly, BChl b_{DHGG} esterified with a 2,10,14-phytatrienyl tail eluted slightly earlier

FIG 4 Legend (Continued)
insertion region shown in GGR (BchP) of *H. halochloris* is colored in red. Important residues close to the substrate-binding site in *Sulfolobus acidocaldarius* GGR crystal structure studies are colored in green. *H.*, *Halorhodospira*; *Ect.*, *Ectothiorhodospira*; *Rvi.*, *Rubrivivax*; *Blc.*, *Blastochloris*; *Alc.*, *Allochromatium*; *Phs.*, *Phaeospirillum*; *Rps.*, *Rhodopseudomonas*; *Tfc.*, *Thioflavicoccus*; *Erb.*, *Erythrobacter*; *R.*, *Rhodobacter*; *Rvu.*, *Rhodovulum*; *Rsb.*, *Roseobacter*; *Rsp.*, *Rhodospirillum*; *C.*, *Chlorobaculum*; *Cfl.*, *Chloroflexus*; *Rof.*, *Roseiflexus*.

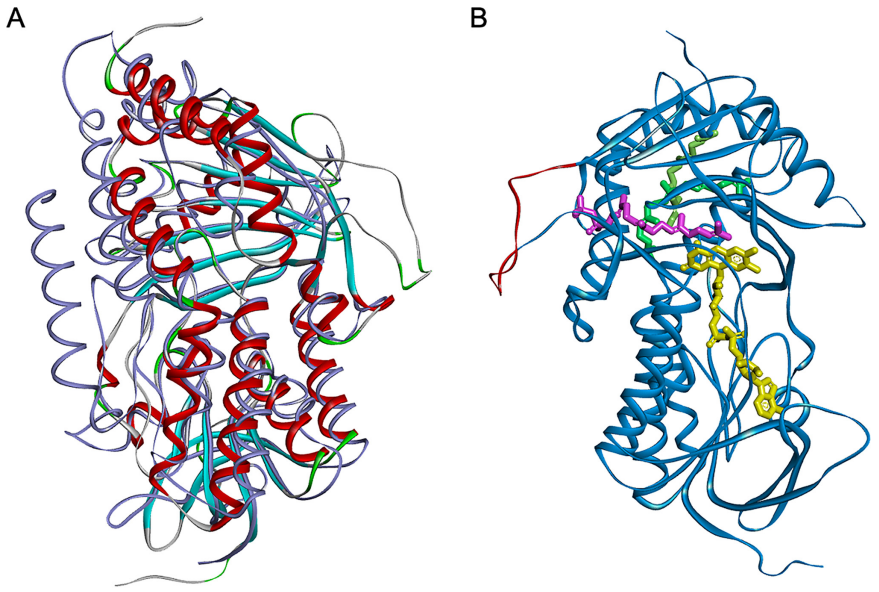

FIG 5 GGR structure prediction with AlphaFold. (A) The predicted structure of *H. halochloris* GGR (colored by secondary structure type) superimposed with the protein structure of *S. acidocaldarius* GGR (colored in gray, 4OPD, ref#22). (B) The predicted structure of *H. halochloris* GGR aligned with FAD (yellow) and three geranylgeranyl pyrophosphates (magenta, green, and light green). Positions of FAD and geranylgeranyl pyrophosphates were extracted from 4OPD after overlaying GGR structures of *H. halochloris* and *S. acidocaldarius*. The substrate geranylgeranyl pyrophosphate (colored in magenta), closest to FAD, locates in the vicinity of the looped insertion region characteristic for *H. halochloris* GGR (colored in red). Protein structure prediction was performed using the ColabFold platform (32), which is based on AlphaFold2 (33). The angle of view in B is horizontally rotated by roughly 180° from that in A.

than BChl b_{DHGG} with a 2,6,14-phytatrienyl tail (16). These suggest that the isoprenoid moieties of BChl a_{THGG} and BChl a_{DHGG} from mutants with *H. halochloris* GGRs would be 2,10-phytadienyl and 2,10,14-phytatrienyl tails, respectively.

MATERIALS AND METHODS

Bacterial strains and culture conditions. *Rhodobacter sphaeroides* J001 strain is a rifampicin-resistant derivative of *R. sphaeroides* 2.4.1 (23) used in this study for genetic manipulations. *R. sphaeroides* strains were cultivated in a PYS medium (24) at 30°C under oxic dark and anoxic light conditions. Furthermore, *Rhodopseudomonas* sp. strain Rits (21) was cultivated in a PYS medium at 30°C under anoxic light conditions. *E. coli* strains were cultivated in a Luria–Bertani (LB) medium at 37°C (25, 26). *H. halochloris* was grown in DSM253 medium at 42°C under anoxic light conditions, as instructed by Deutsche Sammlung von Mikroorganismen und Zellkulturen (DSMZ). Antibiotics were added to the media at the following concentrations: 25 μg/mL kanamycin, 100 μg/mL rifampicin, and 25 μg/mL streptomycin. Table 1 shows the strains and plasmids used in this study.

Construction of *R. sphaeroides* mutants lacking GGR. We amplified the upstream and downstream regions of the *bchP* gene in *R. sphaeroides* by PCR using two primer sets, bchPus-F and bchPus-R, and bchPds-F and bchPds-R, respectively (Fig. 2A, Table 2). The *neo* gene, which confers resistance to kanamycin, was amplified from the plasmid pUCKM1 (27) by PCR using the primer set, neo-F and neo-R (28). Using the In-Fusion HD Cloning Kit (TaKaRa-Bio, Shiga, Japan), we cloned the three amplified PCR products together into the SmaI site of the pJSC suicide vector (29) to obtain plasmid pJSC-bchPKm (Fig. 2A, Table 1).

The plasmid pJSC-bchPKm was transferred into the wild-type strain *R. sphaeroides* using a conjugation method with *E. coli* strain S17-1 *λ-pir* (26, 29). We selected the kanamycin-resistant colonies grown in the presence of 5% sucrose as double-crossover candidates. Then, we performed analytical PCR to verify the chromosomal insertion of the *neo* gene into the *bchP* locus of genomic DNA (Fig. 2A). Using sphaP-comf-F and sphaP-comf-R primers (Table 2), the size of the PCR product from the wild-type strain of *R. sphaeroides* is expected to be 2.48 kbp, which was observed in Fig. 2B, lane 1. The same primer set amplified an approximately 0.18 bp-longer fragment for the mutant strain (Fig. 2B, lane 2). These results indicate that the kanamycin-resistance gene was introduced into the targeted *bchP* gene in the genome of the mutant, which is hereafter called Δ*bchP* mutant.

Complementation mutants carrying wild-type and variant GGR. To construct the mutant complemented with *H. halochloris* GGR, we amplified the *bchP* gene of *H. halochloris* by PCR using primers, HhalbchP-JF and Hhal-bchP-JR (Table 2). Using the In-Fusion technique, we cloned the DNA fragment into the BsaI site of the streptomycin-resistant plasmid vector pJN7 (9) to yield pJ7-HhalbchP. The plasmid was

TABLE 1 Strains and plasmids used in this study[a]

Strain or plasmid	Relevant characteristics	Reference or source
E. coli		
DH5α	Host for cloning vectors	Toyobo Co.
JM109 λ-*pir*	Host of pJSC vector for cloning	25
S17-1 λ-*pir*	Host for pJSC derivatives to deliver to Δ*bchP* strain by conjugation	26
H. halochloris		
DSM 1059	Wild type	DSMZ
R. sphaeroides		
J001 (wild type)	Plating rifampicin resistance derivative from *Rba. sphaeroides* 2.4.1 (Rf^r)	23
Δ*bchP*	*bchP* gene deleted mutant (Rf^r, Km^r)	This study
Hh_P_wt	Δ*bchP* introduced the pJ7-HhalbchP plasmid (Rf^r, Km^r, Sm^r)	This study
Hh_P_del	Δ*bchP* introduced the pJ7-HhalPdel plasmid (Rf^r, Km^r, Sm^r)	This study
Rs_P_wt	Δ*bchP* introduced the pJ7-RsphbchP plasmid (Rf^r, Km^r, Sm^r)	This study
Rs_P_ins	Δ*bchP* introduced the pJ7-RsphPins plasmid (Rf^r, Km^r, Sm^r)	This study
Plasmids		
pUCKM1	pUC plasmid with *neo* gene (Ap^r, Km^r)	27
pJSC	A derivative of suicide vector pJP5603 containing *sacB* and *cat* (Cm^r)	29
pJN7	A derivative of broad-range host vector pBBR1MCS2 to which the *puc* promotor, BsaI restriction site, and Sm^r cartridge are embedded (Km^r, Sm^r)	9
pJSC-bchPKm	(pJSC+*bchP*::neo). Most of the *bchP* coding region of *R. sphaeroides* replaced with *neo* (Cm^r, Km^r)	This study
pJ7-HhalbchP	Intact *bchP* of *H. halochloris* cloned in pJN7 (Km^r, Sm^r)	This study
pJ7-HhalPdel	Variant *H. halochloris bchP* lacking the insertion region cloned in pJN7 (Km^r, Sm^r)	This study
pJ7-RsphbchP	Intact *bchP* of *R. sphaeroides* cloned in pJN7 (Km^r, Sm^r)	This study
pJ7-RsphPins	Variant *R. sphaeroides bchP* having the insertion region derived from *H. halochloris bchP*, cloned in pJN7 (Km^r, Sm^r)	This study

[a]Ap^r, ampicillin resistance; Km^r, kanamycin resistance; Rf^r, rifampicin resistance; Sm^r, streptomycin resistance; Cm^r, chloramphenicol.

transformed into Δ*bchP* mutant by conjugation with the *E. coli* strain S17-1 (29). Transconjugant colonies were selected on PYS plates containing streptomycin (25 μg/mL), kanamycin (25 μg/mL), and rifampicin (100 μg/mL). Colonies were selected from the third round of selective plates and cultivated in a liquid PYS medium. To verify that conjugation was successfully achieved, plasmids were extracted from the liquid cultures and confirmed to be pJ7-HhalbchP by cutting with the appropriate restriction enzymes and amplifying the *bchP* gene. This mutant was designated Hh_P_wt. Note that the introduction of plasmid pJ7-HhalbchP provided the heterologous expression of *H. halochloris bchP* under the transcriptional control of the *puc* operon promoter derived from *R. sphaeroides*.

The mutant complemented with a variant GGR of *H. halochloris*, in which the characteristic insertion region at the N-terminus was deleted, was constructed as follows. DNA fragments containing partial *bchP* gene regions of *H. halochloris* were amplified by PCR using two sets of primers, Hhal-bchP-JF and

TABLE 2 Sequences of primers for construction of the plasmids and confirmation of the mutants used in this study

Primer name	Primer sequence	Sequences for In-Fusion (underlined) overlapped with...
bchPus-F	TCGAGCTCGGTACCCTTCATGCAGGAGCTGATCCT	pJSC, SmaI site
bchPus-R	CGCTTCCTTTAGCAGACGAAGACATCATAGGCCAT	*neo* gene, 5′-end
bchPds-F	TGCTGGAGTTCTTCGCAAGATCGGGTTCAAGAACG	pJSC, SmaI site
bchPds-R	CTCTAGAGGATCCCCTGCAAGCCACAAGAAAAGGG	*neo* gene, 3′-end
neo-F	CTGCTAAAGGAAGCGGAACA	
neo-R	CGAAGAACTCCAGCATGAGA	
sphaP-comf-F	CTTCACCTTCTTCGTCTTCC	
sphaP-comf-F	GACCTCTTGCAAACGCAGAC	
Hhal-bchP-JF	CGAGAAGGGCGGCGCCCCAGTGGCCAATAATTCTGCTG	pJN7, BsaI site
Hhal-bchP-JR	CTGGGTACCGATATCTCAGCTCGAGCGCGCGAGG	pJN7, BsaI site
Hhal-bchP-middleR	GATATCCATGTCAGCATGG	Hhal-bchP-middleAF
Hhal-bchP-middleAF	GCTGACATGGATATCCCCTTGAGCATGCTGAGCATG	Hhal-bchP-middleR
Rsph-bchP-JF	CGAGAAGGGCGGCGCCGCCTATGATGTCTTCGTAGTG	pJN7, BsaI site
Rsph-bchP-JR	CTGGGTACCGATATCTCAGGTCCATTGCGGCGAG	pJN7, BsaI site
Rsph-bchP-insertR[a]	*CTGGCGGAAGGGCCA*CTCCGGGGGCGGGGATCGGG ATGTCGACCTTGC	Rsph-bchP-insertAF
Rsph-bchP-insertAF	*TGGCCCTTCCGCCAG*ACGCCAAAGACGGGGAGGGC GGCTTCGTCGG	Rsph-bchP-insertR

[a]Italicized sequences in Rsph-bchP-insertR and Rsph-bchP-insertAF correspond to the coding region for the inserted peptides.

HhaI-bchP-middleR, and HhaI-bchP-middleAF and HhaI-bchP-JR (Table 2). The two PCR fragments were cloned together into the BsaI site of plasmid pJN7, yielding plasmid pJ7-HhaIPdel. Then, we transferred the plasmid into the Δ*bchP* mutant by conjugation as described above, and the obtained complementation mutant was designated Hh_P_del.

For the control mutant strain complemented with wild-type *R. sphaeroides* GGR, the *bchP* gene of *R. sphaeroides* was amplified by PCR using primers, Rsph-bchP-JF and Rsph-bchP-JR (Table 2). The PCR fragment was cloned into the BsaI site of pJN7 using the In-Fusion method, yielding pJ7-RsphbchP. Then, the plasmid was transferred into the Δ*bchP* mutant by conjugation as described above. The resultant complementation mutant was designated as Rs_P_wt. Also, the complementation mutant with a variant GGR of *R. sphaeroides* was constructed similarly. Additional peptides from the characteristic insertion region of *H. halochloris* GGR was embedded in the variant GGR of *R. sphaeroides* in the mutant. Two DNA fragments containing *bchP* of *R. sphaeroides* front and back from the insertion region were amplified by PCR using two sets of primers: Rsph-bchP-JF and Rsph-bchP-insertR; and Rsph-bchP-insertAF and Rsph-bchP-JR (Table 2). The primers, Rsph-bchP-insertR and Rsph-bchP-insertAF, include sequences corresponding to the coding region for the inserted peptides, PAPGVALPPDAKDG (Table 2). The two fragments were cloned together into the BsaI site of plasmid pJN7 using the In-Fusion method, yielding the plasmid pJ7-RsphPins, and the following conjugation, selection, and genetic verification were conducted as for other complementation mutants. The resultant mutant was designated Rs_P_ins.

HPLC analysis. The wild-type and mutant strains were cultivated in a PYS medium under semi-oxic dark and anoxic light conditions for pigment analysis. Note that *Rhodobacter* species typically accumulate BChl pigments even under dark conditions. The HPLC results depicted in the figure were obtained using pigments extracted from cells grown under dark conditions; however, HPLC analysis using pigments from cells grown under light conditions yielded the same results. We harvested the cells using centrifugation, extracted the pigments with acetone/methanol (7:2, vol/vol), and filtered them with a PVDF membrane. We performed reverse-phase HPLC measurements using an octadecylated silica gel column (Cosmosil $5C_{18}$-AR-II 4.6 mmϕ × 250 mm, 5 μm, Nacalai Tesque, Kyoto, Japan) with a mobile phase, methanol:acetone:water = 82:15:3 with a flow rate of 0.4 mL/min.

ACKNOWLEDGMENTS

We thank Yasuhiro Shimane for his help on performing AlphaFold analysis. This work was partially supported by the Japan Society for the Promotion of Science (JSPS) KAKENHI grant numbers 19H02018 and 18H03743 (to Y.T.) and JP17H06436 in the Scientific Research on Innovative Areas "Innovation for Light-Energy Conversion (I^{4}LEC)" (to H.T.), and by the Astrobiology Center of National Institutes of Natural Sciences (grant number AB021015 to Y.T.).

Y.T. and H.T. designed the research and developed the concept. Y.T., J.H., and H.T. wrote the manuscript. Y.T., J.H., K.K., and K.T. performed the experiments. All authors analyzed the data and discussed the results for completing the manuscript.

REFERENCES

1. van de Meent EJ, Kobayashi M, Erkelens C, van Veelen PA, Amesz J, Watanabe T. 1991. Identification of 8^1-hydroxychlorophyll *a* as a functional reaction center pigment in heliobacteria. Biochim Biophys Acta 1058:356–362. https://doi.org/10.1016/S0005-2728(05)80131-8.
2. Kobayashi M, Oh-Oka H, Akutsu S, Akiyama M, Tominaga K, Kise H, Nishida F, Watanabe T, Amesz J, Koizumi M, Ishida N, Kano H. 2000. The primary electron acceptor of green sulfur bacteria, bacteriochlorophyll 663, is chlorophyll *a* esterified with Δ2,6-phytadienol. Photosynth Res 63:269–280. https://doi.org/10.1023/A:1006480629059.
3. Tsukatani Y, Romberger SP, Golbeck JH, Bryant DA. 2012. Isolation and characterization of homodimeric type-I reaction center complex from *Candidatus* Chloracidobacterium thermophilum, an aerobic chlorophototroph. J Biol Chem 287:5720–5732. https://doi.org/10.1074/jbc.M111.323329.
4. Tamiaki H, Teramura M, Tsukatani Y. 2016. Reduction processes in biosynthesis of chlorophyll molecules: chemical implication of enzymatically regio- and stereoselective hydrogenations in the late stages of their biosynthetic pathway. Bull Chem Soc Jpn 89:161–173. https://doi.org/10.1246/bcsj.20150307.
5. Bryant DA, Hunter CN, Warren MJ. 2020. Biosynthesis of the modified tetrapyrroles—the pigments of life. J Biol Chem 295:6888–6925. https://doi.org/10.1074/jbc.REV120.006194.
6. Nomata J, Mizoguchi T, Tamiaki H, Fujita Y. 2006. A second nitrogenase-like enzyme for bacteriochlorophyll biosynthesis: reconstitution of chlorophyllide *a* reductase with purified X-protein (BchX) and YZ-protein (BchY-BchZ) from *Rhodobacter capsulatus*. J Biol Chem 281:15021–15028. https://doi.org/10.1074/jbc.M601750200.
7. Tsukatani Y, Yamamoto H, Harada J, Yoshitomi T, Nomata J, Kasahara M, Mizoguchi T, Fujita Y, Tamiaki H. 2013. An unexpectedly branched biosynthetic pathway for bacteriochlorophyll *b* capable of absorbing near-infrared light. Sci Rep 3:1217–1217. https://doi.org/10.1038/srep01217.
8. Tsukatani Y, Yamamoto H, Mizoguchi T, Fujita Y, Tamiaki H. 2013. Completion of biosynthetic pathways for bacteriochlorophyll *g* in *Heliobacterium modesticaldum*: the C8-ethylidene group formation. Biochim Biophys Acta 1827:1200–1204. https://doi.org/10.1016/j.bbabio.2013.06.007.
9. Tsukatani Y, Harada J, Nomata J, Yamamoto H, Fujita Y, Mizoguchi T, Tamiaki H. 2015. *Rhodobacter sphaeroides* mutants overexpressing chlorophyllide *a* oxidoreductase of *Blastochloris viridis* elucidate functions of enzymes in late bacteriochlorophyll biosynthetic pathways. Sci Rep 5:9741. https://doi.org/10.1038/srep09741.
10. Bollivar DW, Wang S, Allen JP, Bauer CE. 1994. Molecular genetic analysis of terminal steps in bacteriochlorophyll *a* biosynthesis: characterization of a *Rhodobacter capsulatus* strain that synthesizes geranylgeraniol-esterified bacteriochlorophyll *a*. Biochemistry 33:12763–12768. https://doi.org/10.1021/bi00209a006.
11. Addlesee HA, Fiedor L, Hunter CN. 2000. Physical mapping of bchG, orf427, and orf177 in the photosynthesis gene cluster of *Rhodobacter sphaeroides*: functional assignment of the bacteriochlorophyll synthetase gene. J Bacteriol 182:3175–3182. https://doi.org/10.1128/JB.182.11.3175-3182.2000.
12. Kim E-J, Lee JK. 2010. Competitive inhibitions of the chlorophyll synthase of *Synechocystis* sp. strain PCC 6803 by bacteriochlorophyllide *a* and the bacteriochlorophyll synthase of *Rhodobacter sphaeroides* by chlorophyllide *a*. J Bacteriol 192:198–207. https://doi.org/10.1128/JB.01271-09.

13. Addlesee HA, Hunter CN. 1999. Physical mapping and functional assignment of the geranylgeranyl-bacteriochlorophyll reductase gene, *bchP*, of *Rhodobacter sphaeroides*. J Bacteriol 181:7248–7255. https://doi.org/10.1128/JB.181.23.7248-7255.1999.
14. Tamiaki H, Nomura K, Mizoguchi T. 2017. Preparation of regio- and stereoisomeric di- and tetrahydrogeranylgeraniols and identification of esterifying groups in natural (bacterio)chlorophylls. Bioorg Med Chem 25:6361–6370. https://doi.org/10.1016/j.bmc.2017.10.002.
15. Steiner R, Schäfer W, Bios I, Wieschhoff H, Scheer H. 1981. D2,10-Phytadienol as esterifying alcohol of bacteriochlorophyll *b* from *Ectothiorhodospira halochloris*. Z Naturforsch C 36:417–420. https://doi.org/10.1515/znc-1981-5-613.
16. Mizoguchi T, Isaji M, Harada J, Watabe K, Tamiaki H. 2009. Structural determination of the Δ2,10-phytadienyl substituent in the 17-propionate of bacteriochlorophyll-*b* from *Halorhodospira halochloris*. J Porphyrins Phthalocyanines 13:41–50. https://doi.org/10.1142/S1088424609000218.
17. Harada J, Miyago S, Mizoguchi T, Azai C, Inoue K, Tamiaki H, Oh-oka H. 2008. Accumulation of chlorophyllous pigments esterified with the geranylgeranyl group and photosynthetic competence in the CT2256-deleted mutant of the green sulfur bacterium *Chlorobium tepidum*. Photochem Photobiol Sci 7:1179–1187. https://doi.org/10.1039/b802435a.
18. Chew AGM, Frigaard N-U, Bryant DA. 2008. Identification of the *bchP* gene, encoding geranylgeranyl reductase in *Chlorobaculum tepidum*. J Bacteriol 190:747–749. https://doi.org/10.1128/JB.01430-07.
19. Chen J-H, Wu H, Xu C, Liu X-C, Huang Z, Chang S, Wang W, Han G, Kuang T, Shen J-R, Zhang X. 2020. Architecture of the photosynthetic complex from a green sulfur bacterium. Science 370:eabb6350. https://doi.org/10.1126/science.abb6350.
20. Tsukatani Y, Hirose Y, Harada J, Yonekawa C, Tamiaki H. 2019. Unusual features in the photosynthetic machinery of *Halorhodospira halochloris* DSM 1059 revealed by complete genome sequencing. Photosynth Res 140:311–319. https://doi.org/10.1007/s11120-019-00613-0.
21. Mizoguchi T, Harada J, Tamiaki H. 2006. Structural determination of dihydro- and tetrahydrogeranylgeranyl groups at the 17-propionate of bacteriochlorophylls-*a*. FEBS Lett 580:6644–6648. https://doi.org/10.1016/j.febslet.2006.11.020.
22. Kung Y, McAndrew RP, Xie X, Liu CC, Pereira JH, Adams PD, Keasling JD. 2014. Constructing tailored isoprenoid products by structure-guided modification of geranylgeranyl reductase. Structure 22:1028–1036. https://doi.org/10.1016/j.str.2014.05.007.
23. Harada J, Mizoguchi T, Tsukatani Y, Yokono M, Tanaka A, Tamiaki H. 2014. Chlorophyllide *a* oxidoreductase works as one of the divinyl reductases specifically involved in bacteriochlorophyll *a* biosynthesis. J Biol Chem 289:12716–12726. https://doi.org/10.1074/jbc.M113.546739.
24. Nagashima KVP, Hiraishi A, Shimada K, Matsuura K. 1997. Horizontal transfer of genes coding for the photosynthetic reaction centers of purple bacteria. J Mol Evol 45:131–136. https://doi.org/10.1007/pl00006212.
25. Penfold RJ, Pemberton JM. 1992. An improved suicide vector for construction of chromosomal insertion mutations in bacteria. Gene 118:145–146. https://doi.org/10.1016/0378-1119(92)90263-o.
26. de Lorenzo V, Herrero M, Jakubzik U, Timmis KN. 1990. Mini-Tn5 transposon derivatives for insertion mutagenesis, promoter probing, and chromosomal insertion of cloned DNA in gram-negative eubacteria. J Bacteriol 172:6568–6572. https://doi.org/10.1128/jb.172.11.6568-6572.1990.
27. Saeki K, Suetsugu Y, Tokuda K, Miyatake Y, Young DA, Marrs BL, Matsubara H. 1991. Genetic analysis of functional differences among distinct ferredoxins in *Rhodobacter capsulatus*. J Biol Chem 266:12889–12895. https://doi.org/10.1016/S0021-9258(18)98778-8.
28. Teramura M, Harada J, Mizoguchi T, Yamamoto K, Tamiaki H. 2016. *In vitro* assays of BciC showing $C13^2$-demethoxycarbonylase activity requisite for biosynthesis of chlorosomal chlorophyll pigments. Plant Cell Physiol 57:1048–1057. https://doi.org/10.1093/pcp/pcw045.
29. Simon R, Priefer U, Pühler A. 1983. A broad host range mobilization system for *in vivo* genetic engineering: transposon mutagenesis in gram negative bacteria. Nat Biotechnol 1:784–791. https://doi.org/10.1038/nbt1183-784.
30. Katoh K, Standley DM. 2013. MAFFT multiple sequence alignment software version 7: improvements in performance and usability. Mol Biol Evol 30:772–780. https://doi.org/10.1093/molbev/mst010.
31. Kearse M, Moir R, Wilson A, Stones-Havas S, Cheung M, Sturrock S, Buxton S, Cooper A, Markowitz S, Duran C, Thierer T, Ashton B, Meintjes P, Drummond A. 2012. Geneious Basic: An integrated and extendable desktop software platform for the organization and analysis of sequence data. Bioinformatics 28:1647–1649. https://doi.org/10.1093/bioinformatics/bts199.
32. Mirdita M, Schütze K, Moriwaki Y, Heo L, Ovchinnikov S, Steinegger M. 2021. ColabFold—making protein folding accessible to all. bioRxiv https://doi.org/10.1101/2021.08.15.456425.
33. Jumper J, Evans R, Pritzel A, Green T, Figurnov M, Ronneberger O, Tunyasuvunakool K, Bates R, Žídek A, Potapenko A, Bridgland A, Meyer C, Kohl SAA, Ballard AJ, Cowie A, Romera-Paredes B, Nikolov S, Jain R, Adler J, Back T, Petersen S, Reiman D, Clancy E, Zielinski M, Steinegger M, Pacholska M, Berghammer T, Bodenstein S, Silver D, Vinyals O, Senior AW, Kavukcuoglu K, Kohli P, Hassabis D. 2021. Highly accurate protein structure prediction with AlphaFold. Nature 596:583–589. https://doi.org/10.1038/s41586-021-03819-2.